Supporting Information for

Colloidal CdSe Quantum Wells with Graded Shell Composition for Low-Threshold Amplified Spontaneous Emission and Highly Efficient Electroluminescence

Yusuf Kelestemur,[1,2] Yevhen Shynkarenko,[1,2] Marco Anni,[3] Sergii Yakunin,[1,2] Maria Luisa De Giorgi,[3] and Maksym V. Kovalenko[1,2]*

[1] Department of Chemistry and Applied Biosciences, ETH Zürich, Vladimir Prelog Weg 1, CH-8093 Zürich, Switzerland

[2] Empa − Swiss Federal Laboratories for Materials Science and Technology, Überlandstrasse 129, CH-8600 Dübendorf, Switzerland

[3] Dipartimento di Matematica e Fisica "Ennio De Giorgi", Università del Salento, Via per Arnesano, 73100 Lecce, Italy

[*]Corresponding Author: mvkovalenko@ethz.ch

Table S1. Batch to batch variation of optical properties of CdSe/CdS core/shell NPLs including their PL maximum, FWHM and PLQY.

Sample	PL Max (nm)	FWHM (nm)	PLQY (%)
#1	635	22	48
#2	637	22	56
#3	637	22	52
#4	638	22	46
#5	646	23	60
#6	641	23	58
#7	637	21	55
#8	641	21	60
#9	637	22	58
#10	632	22	59

Table S2. Batch to batch variation of optical properties of CdSe/CdS/$Cd_xZn_{1-x}S$ core/shell NPLs including their PL maximum, FWHM and PLQY.

Sample	PL Max (nm)	FWHM (nm)	PLQY (%)
#1	645	21	85
#2	645	23	80
#3	641	22	89
#4	634	24	75
#5	640	22	86
#6	642	24	80
#7	636	22	75
#8	648	23	82
#9	643	22	77
#10	637	22	76

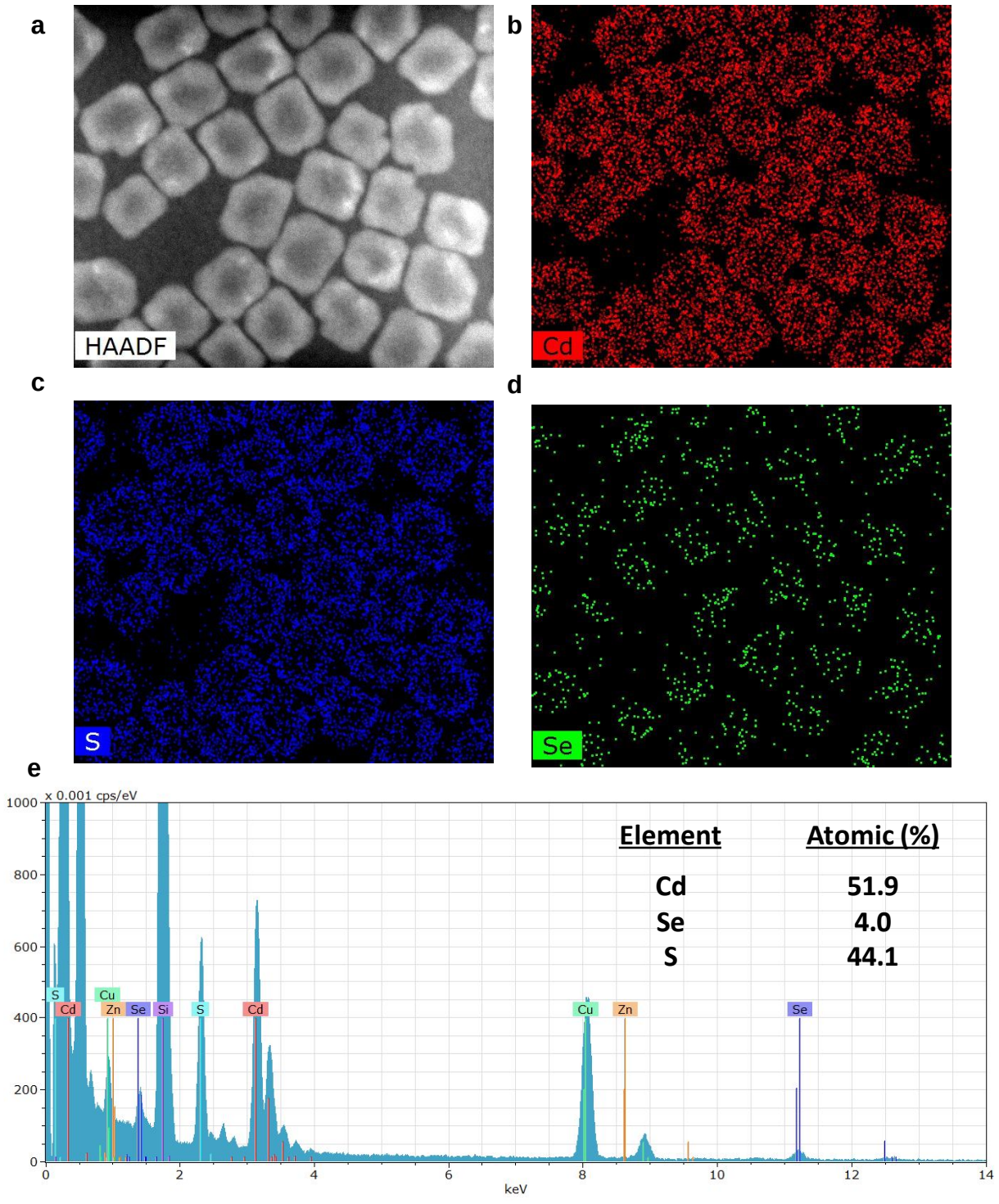

Figure S1. (a) High-angle annual dark-field scanning transmission electron microscopy (HAADF-STEM) image of CdSe/CdS core/shell NPLs and (b-d) their high-resolution elemental mapping. (e) Energy dispersive X-ray spectroscopy (EDS) results of the corresponding image.

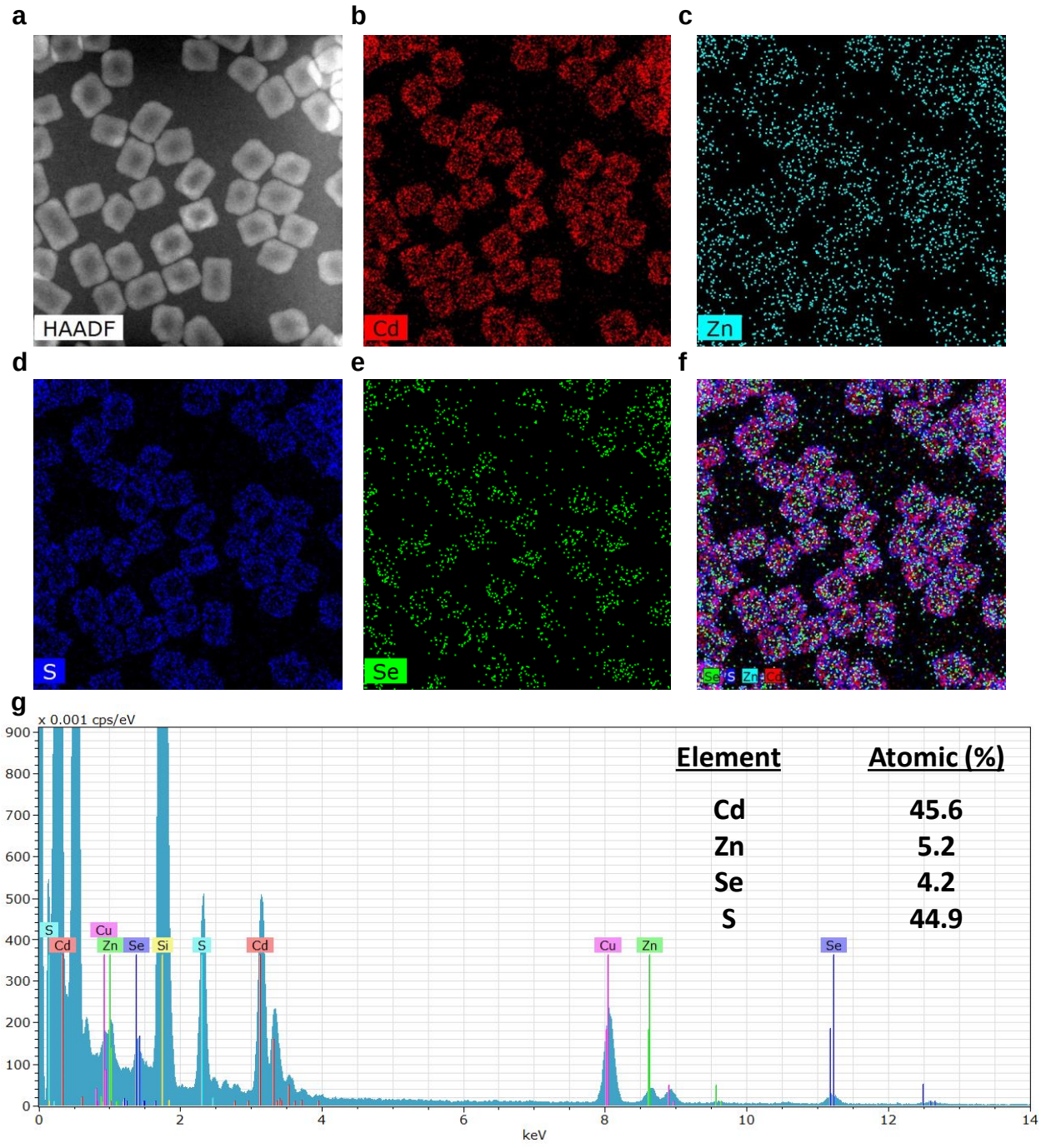

Figure S2. (a) High-angle annual dark-field scanning transmission electron microscopy (HAADF-STEM) image of CdSe/CdS/$Cd_xZn_{1-x}S$ core/shell NPLs and (b-f) their high-resolution elemental mapping. (g) Energy dispersive X-ray spectroscopy (EDS) results of the corresponding image.

Calculation of the Zn to Cd ratio in the shell

For the case of 4 ML CdSe NPLs having four layers of Se and five layers of Cd;

$$\mathrm{Cd(core)} = \mathrm{Se(core)} \times \frac{5}{4} = 5.3$$

$$\mathrm{Cd(total)} = \mathrm{Cd(core)} + \mathrm{Cd(shell)}$$

$$\mathrm{Cd(shell)} = \mathrm{Cd(total)} - \mathrm{Cd(core)} = 40.3$$

the ratio of Zn to Cd in the shell is $\frac{\mathrm{Zn(shell)}}{\mathrm{Cd(shell)}} = \frac{5.2}{40.3} = 0.13$

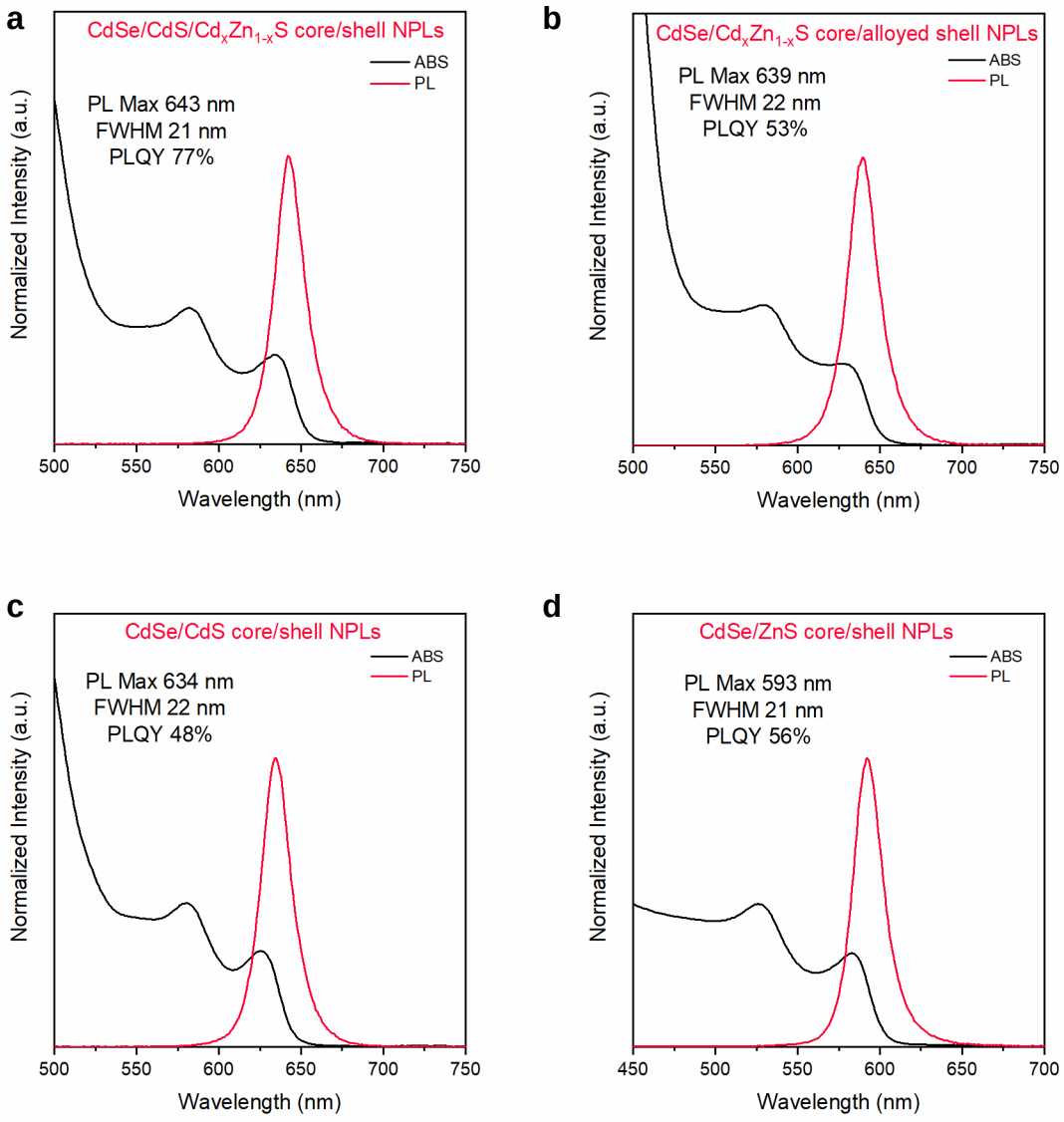

Figure S3. Normalized absorbance and photoluminescence spectra of core/shell NPLs synthesized by using the same CdSe core and having different shell compositions including (a) CdS/$Cd_xZn_{1-x}S$ graded, (b) $Cd_xZn_{1-x}S$ alloyed, (c) CdS and (d) ZnS shell. Core/shell NPLs with CdS/$Cd_xZn_{1-x}S$ graded shell exhibit the highest PLQY among the other core/shell NPLs.

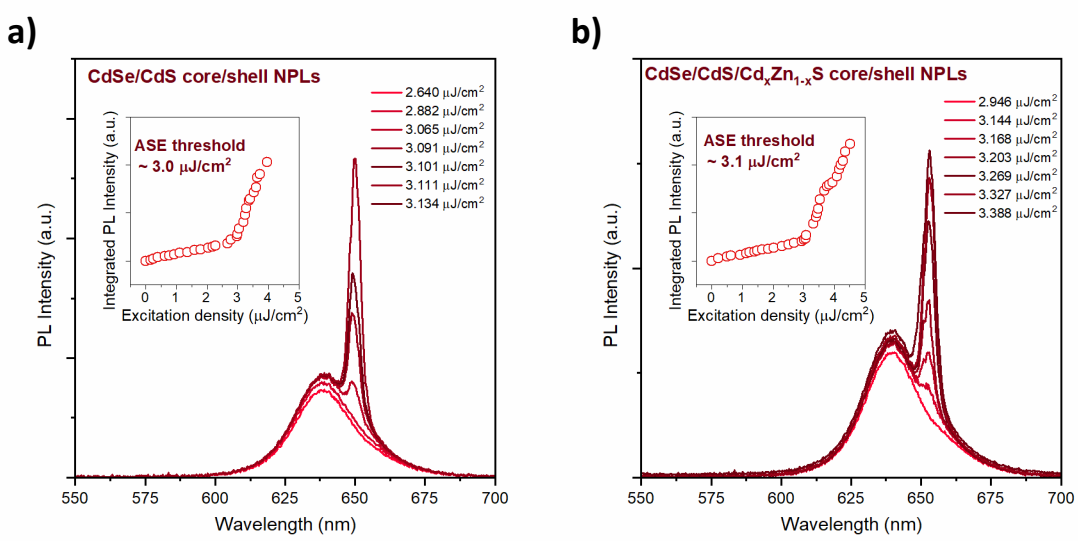

Figure S4. Optical gain performances of core/shell NPLs under femtosecond laser excitation. PL spectra of (a) CdSe/CdS and (b) CdSe/CdS/$Cd_xZn_{1-x}S$ core/shell NPLs at different excitation densities together with the inset showing the integrated PL intensity as a function of excitation density.

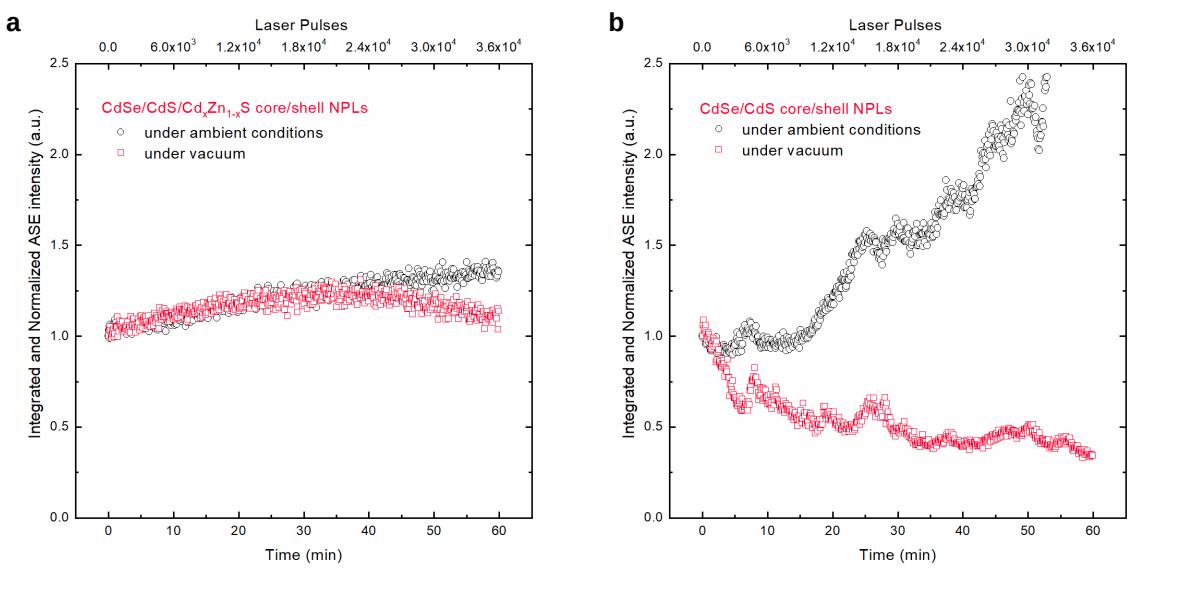

Figure S5. ASE Stability measurements of core/shell NPLs with (a) CdS/$Cd_xZn_{1-x}S$ graded and (b) CdS shell performed under continuous laser excitation at ambient conditions and vacuum. The ASE stability of core/shell NPLs was measured at an excitation density of two-times higher than their ASE thresholds. While CdSe/CdS core/shell NPLs exhibit a continuous degradation in the ASE intensity under vacuum and preserved only ~30% of their initial ASE intensity after 36000 laser pulses (60 min), a strongly improved stability was observed for the NPLs having graded shell in vacuum, showing a small progressive intensity increase in the first 22000 laser pulses (~37 min), followed by a slight degradation. For the stability test performed at ambient conditions, CdSe/CdS core/shell NPLs exhibit a continuously increased ASE intensity, starting after ~10000 laser pulses (17 min) and leading to a 2.4 times higher ASE intensity than the starting one. On the other hand, core/shell NPLs with $Cd_xZn_{1-x}S$ shell showed a stable ASE intensity with a gradually increased ASE with a final intensity of ~25% higher than the starting one. These findings indicate that core/shell NPLs having graded shell yield highly stable ASE performance with reduced sensitivity to any modification on their surfaces during continuous laser pumping. This also supports the proper surface passivation and confinement of excited charge carriers with the additionally grown $Cd_xZn_{1-x}S$ shell, leading to reduced interaction with the surface trap sites.

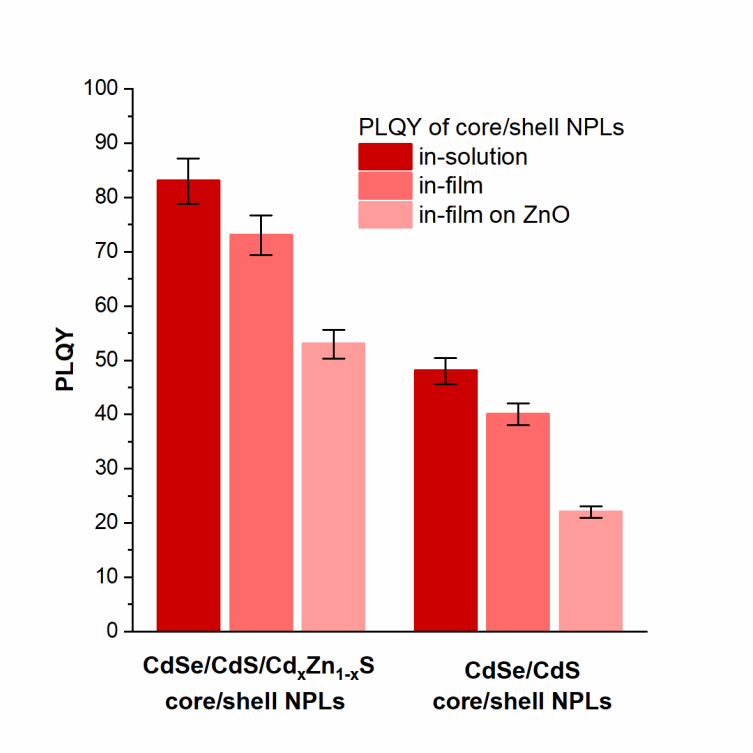

Figure S6. PLQY of core/shell NPLs used for the fabrication of light-emitting-diodes (LEDs). PLQY measurements were performed using the in-solution and in-film samples of colloidal NPLs spin-coated on bare and ZnO coated quartz substrates.

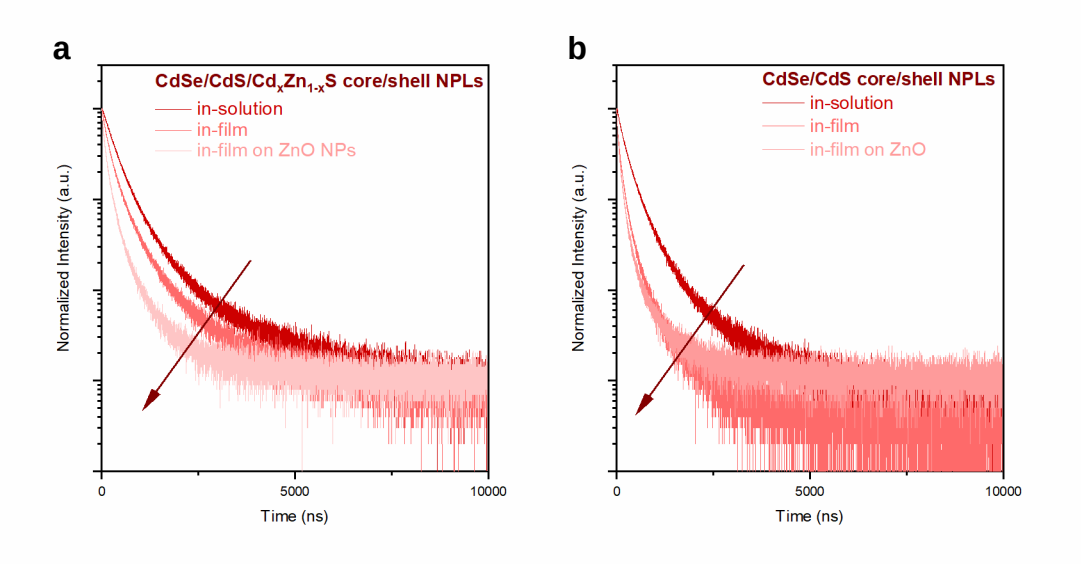

Figure S7. Time-resolved photoluminescence decay curves of core/shell NPLs with (a) CdS/$Cd_xZn_{1-x}S$ graded and (b) CdS shell. The measurements were performed by using the in-solution and in-film samples of colloidal NPLs on bare and ZnO coated quartz substrates.

Table S3. Analysis of time-resolved photoluminescence decay curves of CdSe/CdS/$Cd_xZn_{1-x}S$ core/graded shell NPLs measured by using in-solution and in-film samples of NPLs.

CdSe/CdS/$Cd_xZn_{1-x}S$ core/shell NPLs	*TRF Decay Components*				*Amplitude-average Lifetimes (ns)*
	τ_1	**A_1**	**τ_2**	**A_2**	**τ_{av}**
in-solution	20.64	0.91	72.38	0.11	38.07
in-film	9.44	0.72	35.09	0.28	23.94
in-film on ZnO	3.90	0.62	17.02	0.34	12.34

Table S4. Analysis of time-resolved photoluminescence decay curves of CdSe/CdS core/shell NPLs measured by using in-solution and in-film samples of NPLs.

CdSe/CdS core/shell NPLs	*TRF Decay Components*				*Amplitude-average Lifetimes (ns)*
	τ_1	**A_1**	**τ_2**	**A_2**	**τ_{av}**
in-solution	11.37	0.72	35.58	0.30	26.61
in-film	2.53	0.52	12.53	0.40	9.89
in-film on ZnO	2.55	0.64	11.52	0.31	7.88

Table S5. Literature survey for colloidal NPL-LEDs fabricated by using different heterostructures of colloidal NPLs as an emitter.

Type of NPLs	**Electroluminescence Color**	**EQE_{max} (%)**	**$Luminance_{max}$ (cd/m^2)**
CdSe/CdZnS core/shell NPLs[1]	Red	0.63	4499
CdSe/CdS core/crown NPLs[2]	Green	5	33000
CdSe/CdSeTe core/crown NPLs[3]	Red	3.57	34520
CdSe/CdZnS core/shell NPLs[4]	Red	8.39	1540
CdSeS core NPLs[5]	Green	-	~100
Our study CdSe/CdS/CdZnS core/shell NPL	**Red**	**9.92**	**46000**

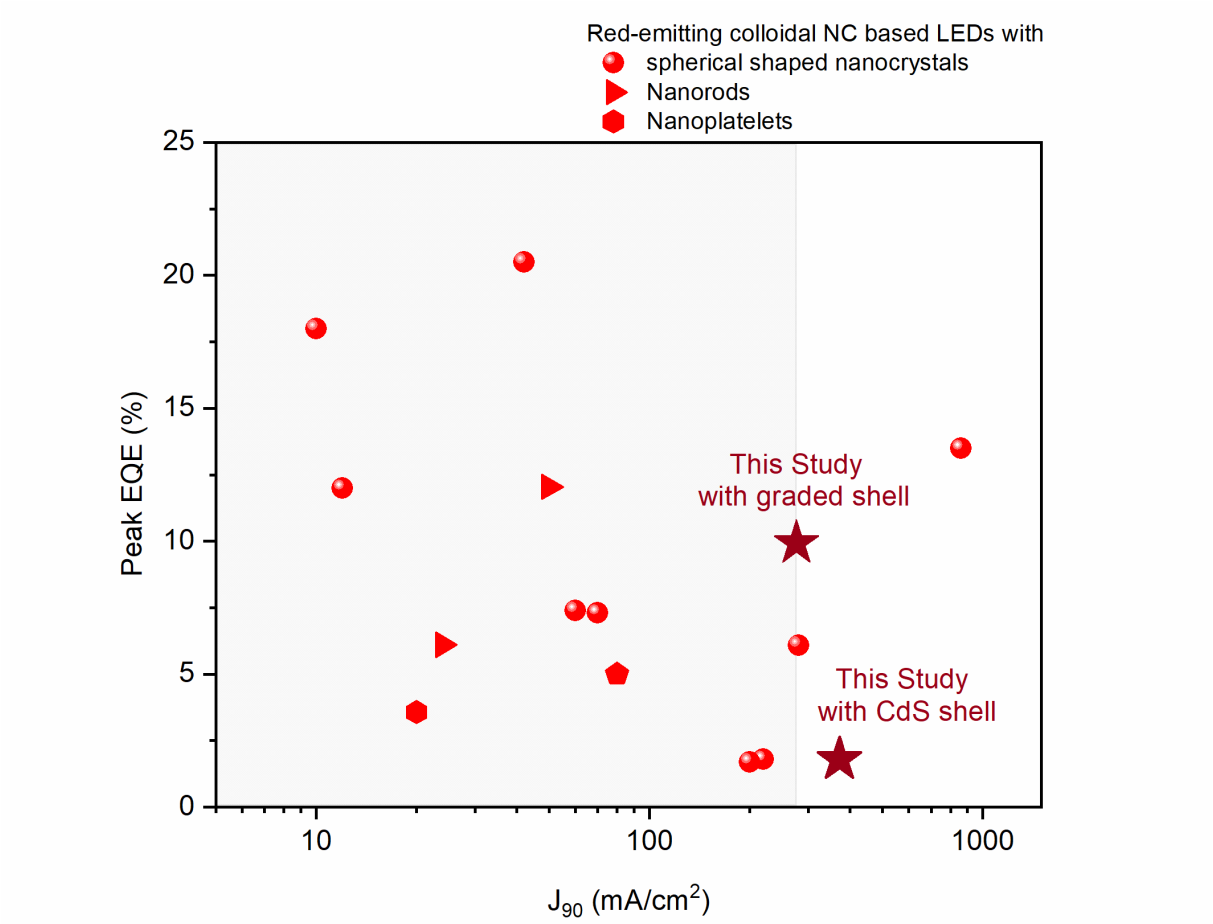

Figure S8. Literature survey of high performance colloidal NC-LEDs having different shell compositions. The graph shows the peak EQE vs J_{90} values of our NPL-LEDs and colloidal NC-LEDs, which are taken from ref. 15.

Table S6. Literature survey of high performance colloidal NC-LEDs having different shell compositions. Peak EQE and J_{90} values of LEDs with core/shell NCs and NRs are taken from ref. 15.

Type of NCs	Electroluminescence Color	EQE_{max} (%)	J_{90} (mA/cm^2)
CdSe/CdS core/shell NCs[6]	Red	20.5	42
CdSe/CdS core/shell NCs[7]	Red	18	10
CdSe/ZnS core/shell NCs[8]	Red	1.7	200
CdSe/CdSeS core/shell NCs[9]	Red	1.8	220
CdSe/CdZnS core/shell NCs[10]	Red	7.4	60
CdSe/CdZnS core/shell NCs[11]	Red	6.09	280
CdSe/CdZnSeS core/shell NCs[12]	Red	12	12
CdSe/CdZnSeS core/shell NCs[13]	Red	7.3	70
CdSe/CdZnSe/ZnS core/shell NCs[14]	Red	13.5	861
CdSe/CdS core/shell NRs[15]	Red	6.1	24
CdS/CdSe/ZnSe Double- heterojunction NRs[16]	Red	12.05	50
CdSe/CdSeTe core/alloyed crown NPLs[3]	Red	3.57	20
CdSe/CdS core/crown NPLs[2]	Green	5	80
Our study CdSe/CdS/CdZnS core/shell NPLs	Red	**9.92**	**276**

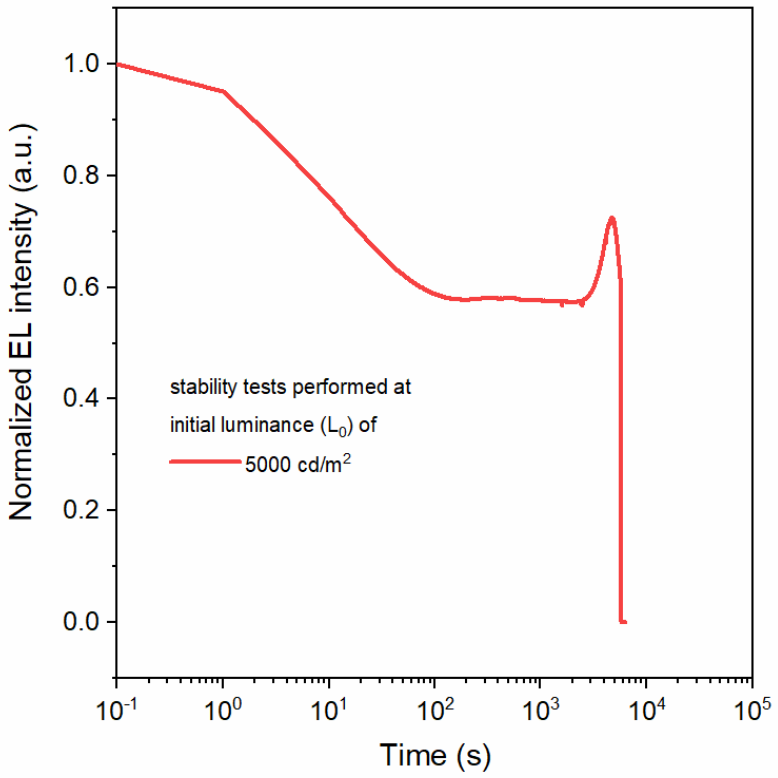

Figure S9. Operational stability of our NPL LEDs. After the encapsulation of devices inside the glovebox, we measured their stability outside the glovebox at ambient conditions. We performed the stability test at constant current density, corresponding to the initial luminance (L_0) of 5000 cd/m^2 and measured the device half-lifetime (T_{50} = 1.6 hr), which is defined as the time duration to observe 50% drop in the luminance. By using the relation of $L_0^n T_{50}$ = constant and assuming an acceleration actor of n = 1.5, we predicted the half-lifetime of our NPL LEDs at 100 cd/m^2 as ~560 hr.

References

(1) Chen, Z.; Nadal, B.; Mahler, B.; Aubin, H.; Dubertret, B. Quasi-2D Colloidal Semiconductor Nanoplatelets for Narrow Electroluminescence. *Adv. Funct. Mater.* **2014**, *24*, 295–302.

(2) Zhang, F.; Wang, S.; Wang, L.; Lin, Q.; Shen, H.; Cao, W.; Yang, C.; Wang, H.; Yu, L.; Du, Z.; Xue, J.; Li, L. S. Super Color Purity Green Quantum Dot Light-Emitting Diodes Fabricated by Using CdSe/CdS Nanoplatelets. *Nanoscale* **2016**, *8*, 12182–12188.

(3) Liu, B.; Delikanli, S.; Gao, Y.; Dede, D.; Gungor, K.; Demir, H. V. Nanocrystal Light-Emitting Diodes Based on Type II Nanoplatelets. *Nano Energy* **2018**, *47*, 115–122.

(4) Giovanella, U.; Pasini, M.; Lorenzon, M.; Galeotti, F.; Lucchi, C.; Meinardi, F.; Luzzati, S.; Dubertret, B.; Brovelli, S. Efficient Solution-Processed Nanoplatelet-Based Light-Emitting Diodes with High Operational Stability in Air. *Nano Lett.* **2018**, *18*, 3441–3448.

(5) Fan, F.; Kanjanaboos, P.; Saravanapavanantham, M.; Beauregard, E.; Ingram, G.; Yassitepe, E.; Adachi, M. M.; Voznyy, O.; Johnston, A. K.; Walters, G.; Kim, G.-H.; Lu, Z.-H.; Sargent, E. H. Colloidal CdSe 1– x S x Nanoplatelets with Narrow and Continuously-Tunable Electroluminescence. *Nano Lett.* **2015**, *15*, 4611–4615.

(6) Dai, X.; Zhang, Z.; Jin, Y.; Niu, Y.; Cao, H.; Liang, X.; Chen, L.; Wang, J.; Peng, X. Solution-Processed, High-Performance Light-Emitting Diodes Based on Quantum Dots. *Nature* **2014**, *515*, 96–99.

(7) Mashford, B. S.; Stevenson, M.; Popovic, Z.; Hamilton, C.; Zhou, Z.; Breen, C.; Steckel, J.; Bulovic, V.; Bawendi, M.; Coe-Sullivan, S.; Kazlas, P. T. High-Efficiency Quantum-Dot Light-Emitting Devices with Enhanced Charge Injection. *Nat. Photonics* **2013**, *7*, 407–412.

(8) Qian, L.; Zheng, Y.; Xue, J.; Holloway, P. H. Stable and Efficient Quantum-Dot Light-Emitting Diodes Based on Solution-Processed Multilayer Structures. *Nat. Photonics* **2011**, *5*, 543–548.

(9) Bae, W. K.; Park, Y.-S.; Lim, J.; Lee, D.; Padilha, L. A.; McDaniel, H.; Robel, I.; Lee, C.; Pietryga, J. M.; Klimov, V. I. Controlling the Influence of Auger Recombination on the Performance of Quantum-Dot Light-Emitting Diodes. *Nat. Commun.* **2013**, *4*, 2661.

(10) Lim, J.; Jeong, B. G.; Park, M.; Kim, J. K.; Pietryga, J. M.; Park, Y.-S.; Klimov, V. I.; Lee, C.; Lee, D. C.; Bae, W. K. Influence of Shell Thickness on the Performance of Light-Emitting Devices Based on CdSe/Zn 1-X Cd X S Core/Shell Heterostructured Quantum Dots. *Adv. Mater.* **2014**, *26*, 8034–8040.

(11) Fokina, A.; Lee, Y.; Chang, J. H.; Braun, L.; Bae, W. K.; Char, K.; Lee, C.; Zentel, R. Side-Chain Conjugated Polymers for Use in the Active Layers of Hybrid Semiconducting Polymer/Quantum Dot Light Emitting Diodes. *Polym. Chem.* **2016**, *7*, 101–112.

(12) Yang, Y.; Zheng, Y.; Cao, W.; Titov, A.; Hyvonen, J.; Manders, J. R.; Xue, J.; Holloway, P. H.; Qian, L. High-Efficiency Light-Emitting Devices Based on Quantum Dots with Tailored Nanostructures. *Nat. Photonics* **2015**, *9*, 259–266.

(13) Kwak, J.; Bae, W. K.; Lee, D.; Park, I.; Lim, J.; Park, M.; Cho, H.; Woo, H.; Yoon, D. Y.; Char, K.; Lee, S.; Lee, C. Bright and Efficient Full-Color Colloidal Quantum Dot Light-Emitting Diodes Using an Inverted Device Structure. *Nano Lett.* **2012**, *12*, 2362–2366.

(14) Lim, J.; Park, Y.-S.; Wu, K.; Yun, H. J.; Klimov, V. I. Droop-Free Colloidal Quantum Dot Light-Emitting Diodes. *Nano Lett.* **2018**, *18*, 6645–6653.

(15) Castelli, A.; Meinardi, F.; Pasini, M.; Galeotti, F.; Pinchetti, V.; Lorenzon, M.; Manna, L.; Moreels, I.; Giovanella, U.; Brovelli, S. High-Efficiency All-Solution-Processed Light-Emitting Diodes Based on Anisotropic Colloidal Heterostructures with Polar Polymer Injecting Layers. *Nano Lett.* **2015**, *15*, 5455–5464.

(16) Nam, S.; Oh, N.; Zhai, Y.; Shim, M. High Efficiency and Optical Anisotropy in Double-Heterojunction Nanorod Light-Emitting Diodes. *ACS Nano* **2015**, *9*, 878–885.